Rational Design of a New Hammerhead Ribozyme Configuration: Lariat Hammerhead Ribozymes as Improved Antisense Therapeutics

Laixin Wang and Duane E. Ruffner*

Contribution from the University of Utah, Department of Pharmaceutics and Pharmaceutical Chemistry, 421 Wakara Way, Suite 318, Salt Lake City, Utah 84108

Received March 9, 1998

Abstract: We have previously shown that circular I/II-format hammerhead ribozymes have faster catalytic rates and a reduced divalent metal-ion requirement.[1,2] The enhanced rate and reduced metal-ion dependence are an asset for in vivo use of hammerhead ribozymes as antisense therapeutics. However, circular hammerheads suffer two disadvantages. Their Km for substrate is increased relative to the wild-type hammerhead, and as I/II-format hammerheads they place greater constraints on the sequences that can be targeted, relative to I/III-format hammerheads. Here we show that these disadvantages can be eliminated in a novel hammerhead configuration, the lariat. The lariat is a I/III-format hammerhead that was constructed by combining chemical and enzymatic methods. The lariat hammerhead ribozyme possesses the same reduced magnesium-ion requirement and enhanced activity of our circular hammerheads. Additionally, the lariat possesses no natural 5′- or 3′-termini and is therefore expected to be of greater resistance to nuclease degradation.

The hammerhead domain is one of the smallest known catalytic oligoribonucleotides. Its small size makes it well suited for study using a wide range of techniques. Consequently, it has become a paradigm for the study of catalytic RNA. As such, it has been the focus of a vast body of work aimed at elucidating its structure and mechanism. In addition to its importance as a model ribozyme, the hammerhead has received much attention due to its potential therapeutic use. Its small size and ability to catalytically cleave a heterologous target RNA make it ideally suited for use as an antisense inhibitor of gene expression. As such, it holds great potential for use in the treatment of disease resulting from aberrant gene expression.

The hammerhead ribozyme is composed of three helices joined at a central conserved core.[3,4] In solution, when divalent metal ions are present, the three helices are arranged in a Y-configuration with helices I and II making up the arms of the Y and helix III forming the single leg.[5−9] This same global conformation is also observed in the crystalline state.[10−12]

Solution studies have indicated that in the absence of divalent metal ions the hammerhead exists in an "open" conformation with helices I and II approximately co-linear and helix III at a 90° angle to helices I and II (Figure 1).[9] With increasing concentration of a divalent metal ion, the open conformation converts to the Y-configuration. As the metal dependence of conversion follows the metal dependence of cleavage, it seems clear that the Y-conformation is the active conformation of the hammerhead.

The conversion from the open to the active conformation has been shown to proceed in two steps, possibly corresponding to the binding of two separate divalent metal ions.[9] The first step involves binding of a metal ion to a low-affinity site that results in a collinear arrangement of helices II and III. This results in the formation of a high-affinity site, likely the site of a catalytic metal ion, that becomes occupied in the second step. Concomitantly, helices I and II become juxtaposed.

The fact that helices I and II are juxtaposed in the active conformation, and that this arrangement requires high concentrations of divalent metal ions, led us previously to examine the activity of circular hammerhead ribozymes (Figure 2).[1,2] These novel hammerheads possess aliphatic linkers connecting helices I and II, effectively constraining the two helices to remain juxtaposed. It was hoped that this would reduce the divalent metal-ion requirement. In fact, when the linker length is optimized, the cleavage activity of the circular ribozyme is greater than that of an equivalent linear ribozyme (Figure 2, HHα5). This increased activity was attributed to a shift in the entire metal ion versus activity profile. This provides support for the Y-conformation and the metal dependence of folding. Additionally, the reduced metal-ion requirement is an asset for in vivo use of hammerheads as antisense therapeutics.

Although the decreased metal-ion dependence is an asset for in vivo use, the circular hammerheads suffer from two disadvantages. First, they are I/II-format hammerheads and therefore place greater restraints on the sequences that can be targeted compared to I/III-format hammerheads. Second, the Km of the circular ribozyme was increased approximately 2-fold. The circular ribozymes, on substrate binding, are subject to an induced twist that likely causes conformational stress in the catalytic core. We suspect that the induced twist may impair

* To whom correspondence should be addressed.

(1) Wang, L.; Ruffner, D. E. Manuscript in prepapration.
(2) Wang, L.; Ruffner, D. E. *Nucleic Acids Res.* **1998**, *26*, 2502−2504.
(3) Forster, A. C.; Symons, R. H. *Cell* **1987**, *49*, 211−220.
(4) Uhlenbeck, O. C. *Nature* **1987**, *328*, 596−600.
(5) Tuschl, T.; Gohlke, C.; Jovin, T. M.; Westhof, E.; Eckstein, F. *Science* **1994**, *266*, 785−789.
(6) Sigurdsson, S. T.; Tuschl, T.; Eckstein, F. *RNA* **1995**, *1*, 575−583.
(7) Bassi, G. S.; Mollegaard, N. E.; Murchie, A. I.; von Kitzing, E.; Lilley, D. M. *Nat. Struct. Biol.* **1995**, *2*, 45−55.
(8) Bassi, G. S.; Murchie, A. I. H.; Lilley, D. M. J. *RNA* **1996**, *2*, 756−768.
(9) Bassi, G. S.; Murchie, A. I. H.; Walter, F.; Clegg, R. M.; Lilley, D. M. J. *EMBO J.* **1997**, *16*, 7481−7489.
(10) Pley, H. W.; Flaherty, K. M.; McKay, D. B. *Nature* **1994**, *372*, 68−74.
(11) Scott, W. G.; Finch, J. T.; Klug, A. *Cell* **1995**, *81*, 991−1002.
(12) Scott, W. G.; Murray, J. B.; Arnold, J. R. P.; Stoddard, B. L.; Klug, A. *Science* **1996**, *274*, 2065−2069.

S0002-7863(98)00796-3 CCC: $15.00
Published on Web 07/25/1998

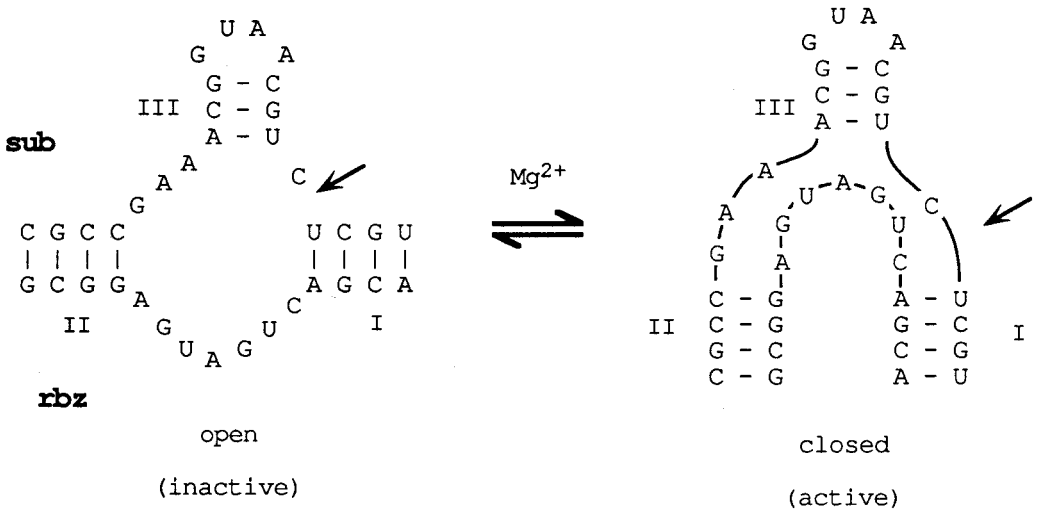

Figure 1. Equilibria between open and closed conformations of the hammerhead ribozyme. Substrate and ribozyme are designated sub and rbz, respectively. The cleavage site is indicated by arrows. Helices I, II, and III are as indicated.

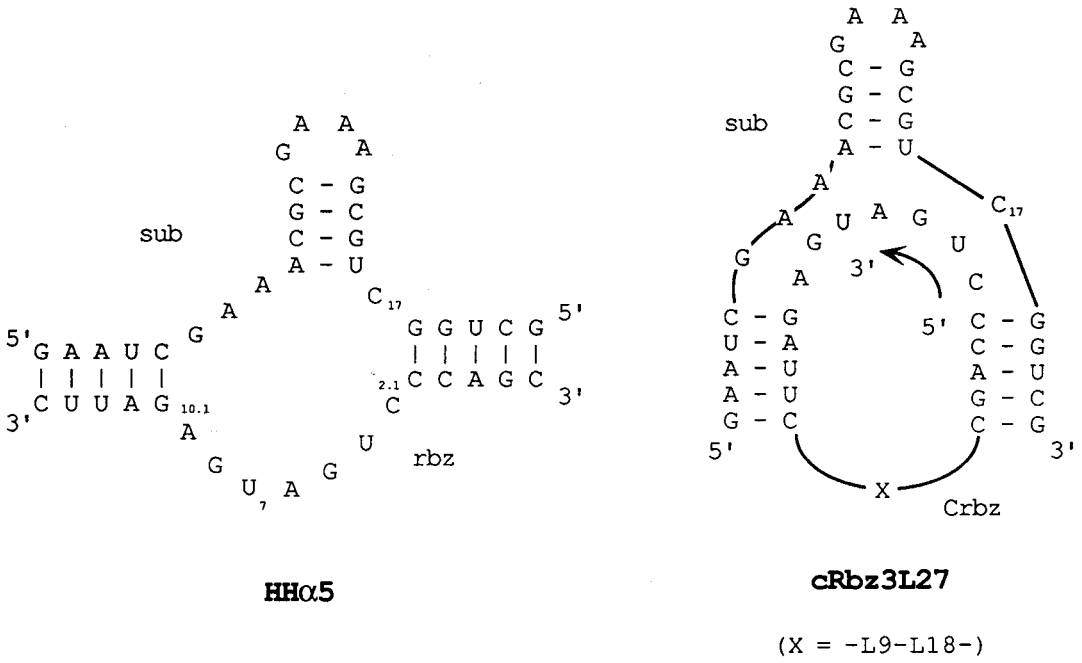

Figure 2. Secondary structures of hammerhead HHα5 and its circular derivative. The composition of X is described in Figure 3.

substrate binding or perturb the active site, and either of these might be responsible for the increase in Km. To overcome the first disadvantage, the circular ribozyme was converted to the I/III format by the addition of an extra arm, thereby creating a "lariat" hammerhead configuration. In an attempt to overcome the Km problem, the lariat ribozyme was synthesized in a manner intended to minimize induced twist.

Results and Discussion

The lariat ribozyme was constructed based on a hammerhead that has been thoroughly characterized kinetically (Figure 2, HHα5).[13] The lariat differs from this hammerhead in that it possesses a non-nucleotide linker in place of loop 2 as well as a non-nucleotide linker connecting helices I and II (Figure 3). The lariat ribozyme was synthesized by combining chemical and enzymatic methods. An amino-terminated (amino-RNA) and a thiol-terminated (thiol-RNA) RNA oligonucleotide were synthesized on an automated DNA synthesizer and used to prepare the lariat ribozyme as illustrated (Figure 4).

The amino-RNA was synthesized with a 3′−3′ inverted deoxyadenosine on the 3′-terminus. This inverted cap prevents the amino-RNA from participating in the ligation reaction in the final step of the lariat synthesis. Synthesis of the lariat was begun by reacting the amino-RNA with excess *N*-(γ-maleimidobutyryloxy) succinimide ester (GMBS, Pierce) to produce the maleimide−RNA adduct (ma−RNA). GMBS was removed by ethyl acetate extraction, and ma−RNA was recovered by ethanol precipitation. The crude ma−RNA product was reacted with the thiol-RNA to produce the branched RNA. Preparative denaturing polyacrylamide gel electrophoresis was used to separate the products of the reaction, and the branched RNA was confirmed by mass spectral analysis. The yield of the branched product was estimated to be 10% based on examination of the gel by UV shadowing. The low yield is surprising on the basis of the known high efficiency of this reaction.[14,15] The basis of the low yield is currently under examination. In

(13) Clouet, D. O. B.; Uhlenbeck, O. C. *RNA* **1996**, *2*, 483−491.

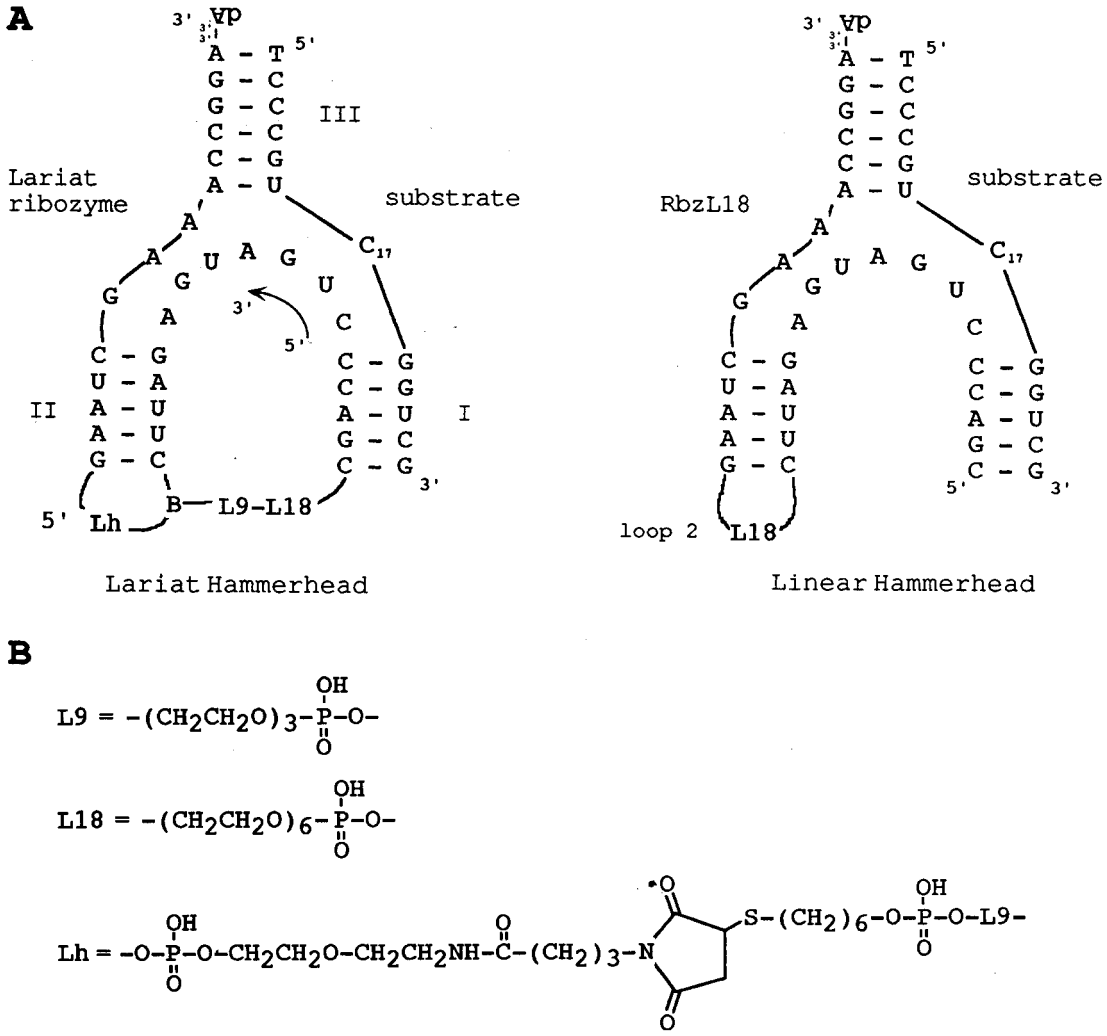

Figure 3. (A) Secondary structures of a lariat and a linear ribozyme. Helices I, II and III are as indicated. (B) Linkers used in the construction of the lariat and linear ribozymes.

the final step, the branched RNA was first annealed to ensure that helix II was preformed. Subsequently, the annealed RNA was reacted with T4 RNA ligase to produce the lariat ribozyme. The lariat product was confirmed by mass spectral analysis. The yield of the lariat was greater than 80%.

For comparison to the lariat ribozyme, a linear homologue was synthesized (Figure 3, RbzL18). An equivalent all RNA ribozyme was also prepared in which a GAAA loop replaced the L18 linker. The cleavage activity of the all RNA ribozyme was indistinguishable from that of RbzL18 (unpublished observation); therefore only RbzL18 was examined further as a control for the lariat ribozyme.

The kinetic parameters k_{cat} and Km were determined for the lariat and linear ribozymes. To ensure that our measured k_{cat} values reflected the rate of the chemical step and not that of product release, the experiments were performed using an excess of ribozyme and a trace amount of radioactive substrate. Since cleavage by the lariat ribozyme at pH 7.5 was too fast to accurately measure, the kinetic analysis was performed at pH 6.5 where the reaction rate has been shown to be approximately 10-fold slower.[16] Under the chosen reaction conditions, cleavage rates were approximately first order for both the lariat and linear ribozymes throughout the first half-life of the reaction at all concentrations examined. Consequently, reaction rates were calculated from the reaction half-lives and subsequently plotted in the form of an Eadie−Hofstee plot (Figure 5).[13,17]

The kinetic parameters k_{cat} and Km were obtained from the Eadie−Hofstee plots (Figure 5 and Table 1). The k_{cat} value for the lariat ribozyme is 2.8 times that for RbzL18, while the Km values are not significantly different. Since k_{cat} is measured under single-turnover conditions, it likely represents the rate of the chemical cleavage. However, it cannot be ruled out that the rate represents rate-limiting substrate binding and/or a rate-limiting conformational change from a ground- to a transition-state structure.

In our previous studies, our circular hammerhead ribozyme cRbz3L27 (Figure 2) exhibited a reduced magnesium-ion requirement compared to the equivalent linear ribozyme. To examine this possibility for the lariat, we examined the single-turnover kinetics of the lariat and linear (RbzL18) ribozymes at magnesium-ion concentrations from 0.05 to 20 mM (Figure 6 and Table 2). Throughout this range the activity of the lariat ribozyme was greater than that of the linear RbzL18. The relative activity was greatest at the lowest concentration examined, where the activity of the lariat was almost 20 times

(14) Kato, Y.; Umemoto, N.; Kayama, Y.; Fukushima, H.; Takeda, Y.; Hara, T. *J. Med. Chem.* **1984**, *27*, 1602−1607.
(15) Shimada, K.; Mitamura, K. *J. Chromatogr. B* **1994**, *659*, 227−241.
(16) Dahm, S. C.; Derrick, W. B.; Uhlenbeck, O. C. *Biochemistry* **1993**, *32*, 13040−13045.
(17) Fedor, M. J.; Uhlenbeck, O. C. *Biochemistry* **1992**, *31*, 12042−12054.

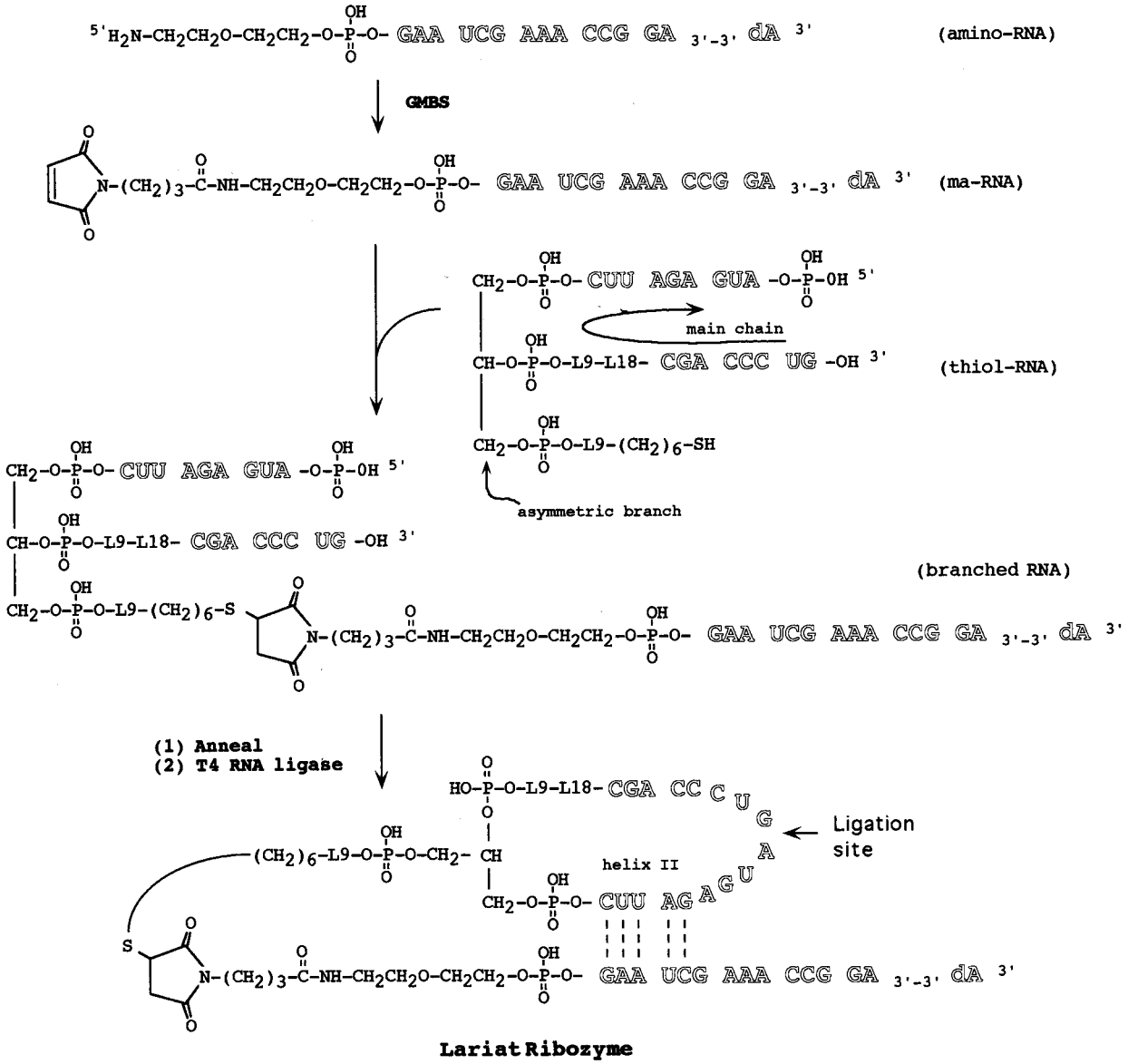

Figure 4. Synthesis of the lariat ribozyme. The sequence of the RNA portion is indicated by open letters. Dashed lines represent the hydrogen bonds produced by Watson−Crick base pairs.

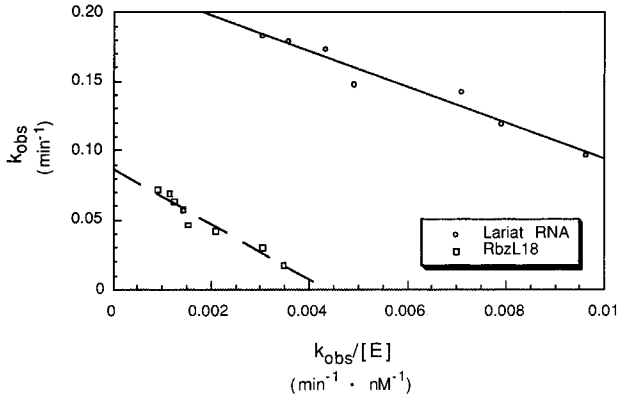

Figure 5. Cleavage kinetics of the lariat and linear ribozymes.

greater than that of RbzL18 (Table 2). The measured cleavage rates likely reflect the rate of the cleavage step, since the relative rate of 2.5 at 10 mM magnesium ion is approximately the same as k_{rel} determined at the same metal-ion concentration (Table 1).

These results further corroborate our previous finding that helix I/II-constrained ribozymes possess catalytic activity,

Table 1. Kinetic Parameters for RbzL18 and the Lariat Ribozyme[a]

ribozyme	k_{cat} (min^{-1})	Km (nM)	k_{cat}/Km (min^{-1} nM)	k_{rel}	relative k_{cat}/Km
lariat	0.24 ± 0.011	14.6 ± 1.8	0.016	2.8	3.6
RbzL18	0.087 ± 0.0045	19.9 ± 2.1	0.0044		

[a] Experiments were performed with ribozyme in excess at pH 6.5 and 25 °C.

activity that can surpass that of normal linear hammerhead ribozymes. The observed enhanced cleavage rates can likely be attributed to one of two inter-related factors. First, by covalently constraining helices I and II, the hammerhead ribozyme is locked into a conformation more closely related to a closed, transition-state-like conformation. This is in contrast to the linear ribozyme that exists in an equilibrium state that favors an open, ground-state conformation. For the linear ribozyme a high divalent metal-ion concentration is required to shift the equilibrium toward the closed conformation. Second, for the linear ribozyme, a catalytic metal-ion binding site is likely to be a transient feature existing only in the closed conformation. In this case, the overall affinity of the site for

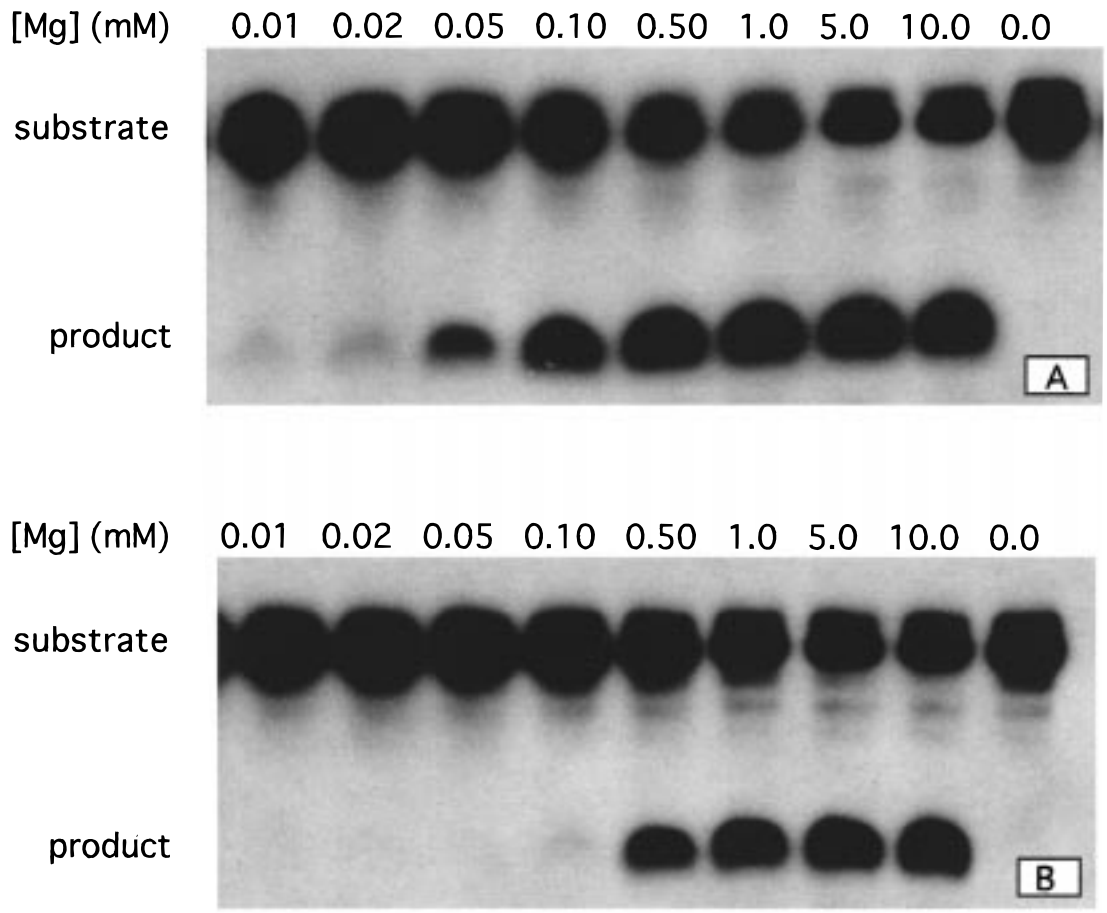

Figure 6. Magnesium-ion dependence of cleavage of lariat (A) and linear (B) ribozymes. Reactions contained 50 mM Tris−HCl (pH 7.5), 100 nM ribozyme, 60 nM substrate (including trace amount 5′-end labeled with ^{32}P), and 0.1% SDS. The reactions were preannealed by incubation at 90 °C for 1.0 min, followed by cooling to room temperature naturally for at least 15 min. The reactions were initiated by addition of magnesium chloride at a concentration varying from 0 to 10 mM, as indicated. Reactions were incubated at room temperature for 30 min and stopped by addition of 2 vols of stop mix (10 mM EDTA/0.02% bromphenol blue and xylene cyanole dye/80% formamide). The reactions were analyzed by fractionation in a denaturing 20% polyacrylamide gel. The gel was visualized by autoradiography.

Table 2. Cleavage Rate vs Magnesium-Ion Concentration for RbzL18 and the Lariat Ribozyme

	k_{obs} (min^{-1})		relative activity
[Mg] (mM)	lariat	RbzL18	lariat/RbzL18
0.05	0.034	*a*	
0.10	0.055	0.0026	18
0.20	0.085	0.0057	14
0.50	0.27	0.039	6.9
1.0	0.36	0.076	4.7
2.0	0.46	0.12	3.8
5.0	0.99	0.33	3.0
10.0	1.4[b]	0.57	2.5
20	1.8[b]	0.8	2.3

[a] No significant amount of product could be detected. [b] The data are approximate because the cleavage is too fast to get precise data using manual pipetting.

the catalytic metal ion is expected to be low, as it reflects binding of the catalytic metal ion to both the open and closed conformations. This is compatible with the observation of Peracchi et al.[18] that the binding affinity of an essential metal ion is low in the ground state but high in the transition state. Since our constrained ribozymes favor a transition-state-like conformation, a high-affinity catalytic metal ion binding site is more likely to be a stable feature, hence the reduced magnesium-ion requirement.

In contrast to our circular ribozymes, Km for the lariat ribozyme is slightly reduced relative to that for the linear ribozyme. This may seem surprising as the lariat is simply a variation of our circular ribozymes, which have previously been shown to possess Km values greater than those of their linear counterparts.[1] We believe this is due to the manner in which the lariat ribozyme was constructed. We previously proposed that the increased Km of the circular ribozyme was a consequence of the circularization. When substrate binds to a circular ribozyme, it induces conformational stress in the circular molecule. This conformational stress could alter substrate binding affinity and/or perturb the structure of the catalytic domain. Either one might affect the measured Km of the reaction. To minimize the potential effect of the conformational stress, a synthetic strategy was chosen for the lariat ribozyme such that helix II would be preformed prior to circularization (Figure 4). Therefore, formation of helix II does not produce conformational stress on the circular portion of the ribozyme. In this case, the lariat is subject to only half the conformational stress of a circular ribozyme, which is induced on formation of helix I. Of course, if we chose to synthesize the lariat by first producing a circular ribozyme and then attaching the lariat tail, we expect that the Km for the lariat ribozyme would be increased relative to its linear homologue, since the circular portion of the lariat would be subject to the same degree of conformational stress experienced by our circular hammerheads.

(18) Peracchi, A.; Beigelman, L.; Scott, E. C.; Uhlenbeck, O. C.; Herschlag, D. *J. Biol. Chem.* **1997**, *272*, 26822−26826.

The influence of conformational stress on I/II-constrained ribozymes may impact on another aspect of circularized ribozymes. The degree of stress can determine the length of linker required to achieve optimal activity. We previously observed that the optimal linker length for circular ribozymes was $\geq$45 Å.[1] In the crystal structure of the hammerhead, helices I and II are separated by approximately 25 Å. We proposed that the discrepancy was due to the linkers performing two roles, establishing optimal separation of helices I and II, and buffering the conformational stress induced by substrate binding. If this is true, we expect that the optimal linker length will be shorter for lariat versus circular ribozymes. While this remains to be tested, the observed kinetic parameters for cRbz3L27 and the lariat ribozyme are compatible with this belief. Both ribozymes possess five base-pair helices I and II, and the same 45 Å linker connecting helices I and II. For both the lariat and cRbz3L27,[1] the k_{cat} values are improved relative to their linear homologues (k_{rel} = 2.8 and 1.5 for the lariat and cRbz3L27, respectively). In contrast, the Km for cRbz3L27 was approximately 2-fold greater than the equivalent linear ribozyme, while the lariat ribozyme has a Km that is mildly reduced compared to its linear homologue. This is likely a consequence of the reduced conformational stress experienced by the lariat ribozyme on substrate binding.

With respect to the clinical application of ribozymes as antisense therapeutics, the lariat ribozyme has significant advantages over wild-type linear ribozymes. First, it possesses higher catalytic activity and comparable substrate binding affinities compared to linear ribozymes. Second, and most significantly, the lariat has a reduced divalent metal-ion requirement. It has been estimated that the total intracellular magnesium-ion concentration is in the range 1−10 mM,[19,20] and much of this is likely to be chelated by polyphosphates such as nucleotide triphosphates and the polynucleotides. The actual free magnesium-ion concentration is likely to be much lower. Our lariat ribozyme exhibits significant activity even at low magnesium concentrations, in contrast to the linear ribozyme. Third, the lariat is likely to be more stable against nuclease degradation. It has no natural free 3′- and 5′-termini, and some nucleotide residues are replaced by non-nucleotide linkers (i.e., loop 2). Fourth, helix I/II-constrained ribozymes such as the lariat are less likely to misfold into inactive conformations, and are expected to exist in a mostly preformed and active state. In this regard, helix I/II-constrained ribozymes will likely be useful in structure/function studies. Finally, the lariat ribozyme is a I/III-format ribozyme. Consequently, it places the fewest requirements on the sequences that can be targeted.

In conclusion, we have synthesized a lariat RNA that has trans-acting ribozyme cleavage activity. The two-piece protocol allows efficient synthesis of the precursor RNAs on a DNA synthesizer, and performing circularization as the last step helps to solve the potential conformational stress problem resulting from association of ribozyme and substrate. As a result of the enhanced performance and the likely lower propensity to misfold, the lariat hammerhead ribozyme offers significant advantages for use in structure/function studies and antisense gene inhibition.

Experimental Section

Synthesis of Oligoribonucleotides. Linear precursor RNAs were synthesized on an ABI 394 DNA synthesizer on a 1.0 μmol scale using the standard phosphoramidite method except where indicated. Spacer 9, spacer 18, 5′-amino-modifier 5 and thio-modifier C6 S-S phosphoramidites, and dA-5′-CPG 500 support were from Glen Research. Asymmetric branching phosphoramidite was from Clontech. Other standard synthesis reagents were from Applied Biosystems Inc. For the amino-RNA, synthesis was begun on a 5′-support (dA-5′-CPG 500). Subsequently, synthesis was performed in a 3′−5′ direction using standard phosphoramidites. Synthesis was completed by the addition of 5′-amino modifier 5 phosphoramidite in the final cycle. Thiol-RNA was synthesized routinely in a 3′−5′ direction using standard reagents, beginning with the main chain (Figure 4). Synthesis continued through the asymmetric branch (asymmetric branching phosphoramidite) by way of the trityl terminated arm. After completion of the main chain, the Lev group on the second arm of the branch was deprotected using hydrazine, and a linker 9 and a C6 S-S thiol modifier were added. After deprotection and purification the thiol-RNA was isolated as a protected disulfide. Both amino-RNA and the protected thiol-RNA were purified using 20% denaturing polyacrylamide gel electrophoresis (PAGE) and were recovered from gels by a crush and soak method. The RNA was concentrated by ethanol precipitation. The oligonucleotide pellets were dissolved in water and stored at −20 °C.

Synthesis of Lariat RNA. The amino-RNA (70 nmol) was reacted with excess *N*-(γ-maleimidobutyryloxy) succinimide ester (GMBS, 700 nmol) in 300 μL of 20 mM phosphate buffer (pH 7.0). The reaction mixture was incubated at room temperature for 5 h, and excess GMBS and its hydrolysis product were removed by ethyl acetate extraction (4 × 300 μL). The reaction products were precipitated with ethanol. The crude product was dissolved in 100 μL of water for reaction with freshly produced thiol-RNA. Thiol-RNA was obtained by reducing the disulfide-protected thiol-RNA with dithiothreitol (DTT). At room temperature 140 nmol of protected RNA was treated with 0.2 M DTT in 300 μL of 50 mM Tris−HCl (pH 8.0) for 2 h. Unreacted DTT was removed by ethyl acetate extraction (4 × 300 μL), and the deprotected thiol-RNA was recovered by ethanol precipitation. The crude thiol-RNA pellet was dissolved in 100 μL of water and immediately combined with the 100 μL of solution of ma−RNA. To this, 4.0 μL of 1.0 M phosphate buffer (pH 7.0) was added, and the reaction mixture was incubated at room temperature for 5 h. The oligonucleotides were ethanol precipitated and fractionated on a denaturing 15% polyacrylamide gel. The gel was visualized by UV shadowing, and only one product was observed. The product, as well as the unreacted precursor RNAs, was recovered from the gel by the crush and soak method. The product was confirmed to be the branched RNA by mass spectral analysis (MALDI-TOF MS: measured *m*/*z* 11 741.6; calculated Mw11 746.4). The mass spectrum was recorded on a Voyager-DE STR Biospectrometry Workstation (PerSeptive Biosystem Inc.) calibrated using protein standards.

The branched RNA was dissolved in 80 μL of water with 13 mM $MgCl_2$. The mixture was heated at 70 °C for 4 min and incubated at 16 °C for 2 h to allow annealing of helix II (Figure 4). To the annealing reaction, 4.0 μL of 10 units/μL T4 RNA ligase, 10.0 μL of 10X buffer (0.5 M Tris−HCl (pH 7.7)/0.1 M DTT), 10.0 μL of 400 mg/mL PEG 8000, and 2.5 μL of 20 mM ATP were added. The reaction mixture was incubated at 16 °C for 18 h. The crude RNA product was obtained by ethanol precipitation and fractionated in a denaturing 15% polyacrylamide gel. Only one RNA band could be observed by UV shadowing. Its mobility was faster than that of the control branched RNA. The product was recovered by the crush and soak method and concentrated by ethanol precipitation. The pellet was dissolved in 60 μL of water and stored at −20 °C. The product was confirmed to be the desired lariat by MALDI-TOF mass spectrometry (MS: *m*/*z* measured 11721.6; calculated Mw 11728.4).

Magnesium Dependence of Cleavage Rates of the Lariat and the Linear Ribozymes. The reactions were performed at room temperature in 25 μL of 50 mM Tris−HCl (pH 7.5) which contained 60 μM ribozyme and 30 μM substrate (with trace amount of ^{32}P-labeled substrate as probe). The reactions were treated with a preannealing step consisting of incubation at 90 °C for 1.0 min, followed by cooling to room temperature naturally for at least 10 min. The reactions were initiated at room temperature by addition of magnesium chloride to a final concentration as indicated in Table 2. Aliquots (about 3 μL) were removed and stopped with the addition of 5 vol of stop mix (30 mM

(19) Lehninger, A. L. *Principles of Biochemistry*; Worth Publishers: New York, 1982.

(20) Sperelakis, N. *Cell Physiology Source Book*; Sperelakis, N., Ed.; Academic Press: New York, 1995.

EDTA/0.02% bromphenol blue and xylene cyanole dye/80% formamide) at times varying from 10 s to 30 min. The samples were electrophoresed in 20% denaturing polyacrylamide gels and analyzed on a Molecular Dynamics phosphorimager. The cleavage rate constants were pseudo-first-order in the first half-life of the reactions. In extended reactions the final extent of cleavage reached 70−85% for both lariat and linear ribozymes. The half-lives were obtained by choosing at least three data points with the cleavage percentage below 30% at each magnesium concentration. The observed cleavage rate constants were calculated using $k_{obs} = 0.693/t_{1/2}$.

Michaelis−Menton Cleavage Kinetics of the Lariat and the Linear Ribozymes. Cleavage reactions were carried out under single-turnover conditions. Reactions were performed in 25 μL of 50 mM Mes (pH 6.5)/0.1% SDS containing a trace amount (less than 2 nM) of ^{32}P-labeled substrate and a series of ribozyme concentrations between 20 and 80 nM. Reactions were preannealed by incubation at 90 °C for 1 min, followed by cooling to room temperature over at least 10 min. The reactions were initiated at room temperature by addition of magnesium chloride to a final concentration of 10 mM. Aliquots (about 3 μL) were removed and added to 10 μL of stopping mix (0.02% xylene/0.02% bromphenol blue/10 mM EDTA/80% formamide) at varying times from 10 s to 15 min such that the extent of cleavage was less than 50%. All samples were electrophoresed in denaturing 20% polyacrylamide gels and the gels were analyzed on a Molecular Dynamics phosphorimager. The cleavage rates were calculated as described above. Km and k_{cat} were obtained from Eadie−Hofstee plots (Figure 5).[17]

Acknowledgment. We are grateful to Dr. James McCloskey for assistance with the mass spectral analysis. Mass spectral analysis was performed by the University of Utah Mass Spectrometry Service Facility. We thank Robert Schackmann of the Huntsman Cancer Institute DNA/Peptide core facility for synthesis of DNA and RNA oligonucleotides. The DNA/Peptide core facility and the Mass Spectrometry Service Facility are supported by a grant from the NIH to the Huntsman Cancer Institute (CA42014). This work was supported by a grant from the NIH to D.E.R., 5R29AI34278.

JA980796Q